

## Herbi Dreiner – University of Bonn

### Nucleon decay in the R-parity violating MSSM

#3

Nidal Chamoun (HIAST), Florian Domingo (U. Bonn, Phys. Inst., BCTP), Herbert K. Dreiner (U. Bonn, Phys. Inst., BCTP)  
(Dec 21, 2020)

Published in: *Phys.Rev.D* 104 (2021) 1, 015020 • e-Print: [2012.11623](#) [hep-ph]

### Decays of a bino-like particle in the low-mass regime

†

Florian Domingo (Bonn U. and U. Bonn, Phys. Inst., BCTP), Herbi K. Dreiner (Bonn U. and U. Bonn, Phys. Inst., BCTP)  
(May 17, 2022)

Published in: *SciPost Phys.* 14 (2023) 5, 134, *SciPost Phys.* 14 (2023) 134 • e-Print: [2205.08141](#) [hep-ph]

### A novel proton decay signature at DUNE, JUNO, and Hyper-K

#

Florian Domingo (Bonn U.), Herbi K. Dreiner (Bonn U.), Dominik Köhler (Bonn U.), Saurabh Nangia (Bonn U.), Apoorva Shah (Bonn U.) (Mar 27, 2024)

Published in: *JHEP* 05 (2024) 258 • e-Print: [2403.18502](#) [hep-ph]

# Proton Decay

- **1954** first experimental proton decay search: Reines, Cowan & Goldhaber

- PDG quotes limits on

$$p \rightarrow \begin{cases} 1 \text{ (anti)lepton + meson(s),} \\ 1 \text{ antilepton + photon(s),} \\ 1 \text{ antilepton + single massless particle,} \\ 3 \text{ or more leptons} \end{cases}$$

- Our proposal:

$$p \rightarrow K^+ + X^0,$$

$$X^0 \rightarrow \{\pi^\pm + \mu^\mp, \pi^0 + \nu_\mu, \pi^0 + \bar{\nu}_\mu\}.$$

$$m_{X^0} \leq m_p - m_{K^+} \approx 445 \text{ MeV}$$

- Here  $X^0 = \tilde{\chi}_1^0$ , but could also have heavy neutral lepton, for example

# Lightest Neutralino can be arbitrarily light

## Mass Bounds on a Very Light Neutralino

Herbi K. Dreiner (Bonn U.), **Sven Heinemeyer** (Cantabria Inst. of Phys.), Olaf Kittel (Granada U., Theor. Phys. Astrophys.), Ulrich Langenfeld (DESY, Zeuthen), Arne M. Weber (Munich, Max Planck Inst.) et al. (Jan, 2009)

Published in: *Eur.Phys.J.C* 62 (2009) 547-572 • e-Print: [0901.3485 \[hep-ph\]](#)

## Neutralino Decays

$$\left. \begin{array}{ll}
 L_i L_j \bar{E}_k : & \tilde{\chi}_1^0 \rightarrow \ell_i^\pm \ell_k^\mp \nu_j \\
 \\ 
 L_i Q_j \bar{D}_k : & \tilde{\chi}_1^0 \rightarrow \ell_i^\pm + 2 \text{ jets} \\
 \\ 
 & \tilde{\chi}_1^0 \rightarrow M_{jk}^\pm + \ell_i^\mp, \quad M_{jk}^0 + \nu_i
 \end{array} \right\} \quad \begin{array}{l}
 \text{for both, for } j=k: \\
 \tilde{\chi}_1^0 \rightarrow \gamma + \nu_i
 \end{array}$$
  

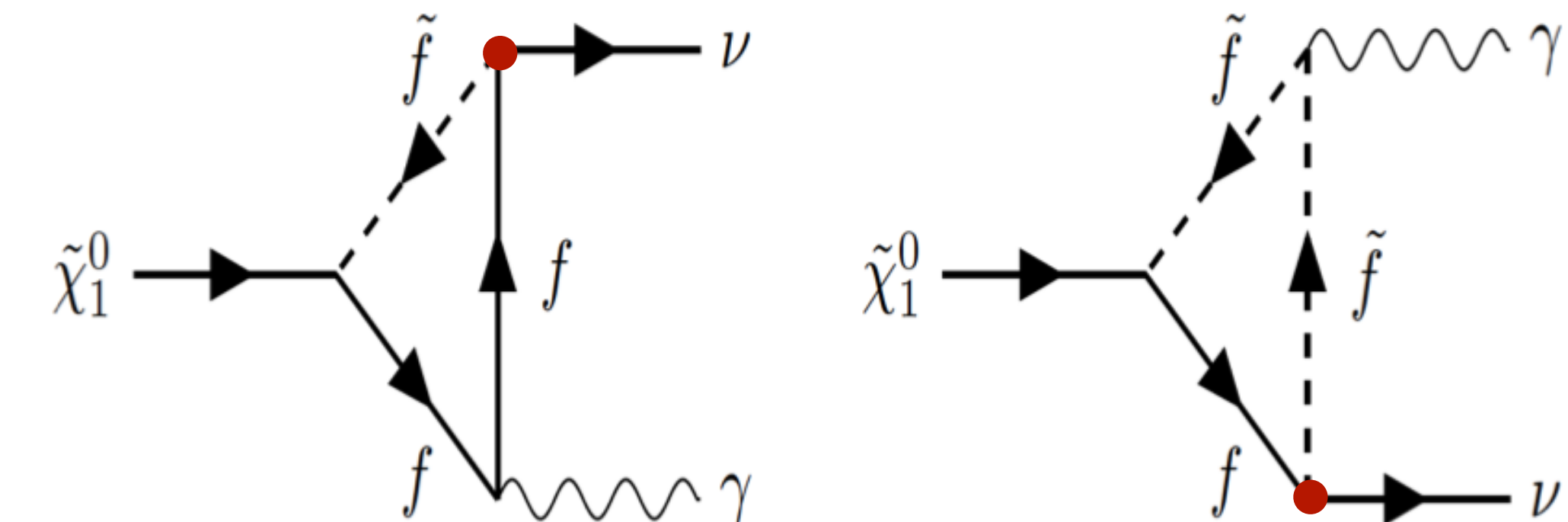
$$\bar{U}_i \bar{D}_j \bar{D}_k : \quad \begin{array}{l}
 \tilde{\chi}_1^0 \rightarrow 3 \text{ jets} \\
 \\ 
 \tilde{\chi}_1^0 \rightarrow M_a B_b \qquad \qquad M_i \in \{\pi^0, \pi^+, \pi^-, K^0, \bar{K}^0, K^+, K^-, \eta_8^0\} \\
 \\ 
 \qquad \qquad \qquad B_j \in \{\Sigma^0, \Sigma^+, \Sigma^-, n^0, \Xi^0, p^+, \Xi^-, \Lambda^0\}
 \end{array}$$

(neutralino can mix with baryon octet)

# Radiative Neutralino Decay

Köhler, Nangia, Wang, HD: *JHEP* 02 (2023) 120

- Novel single photon signature:

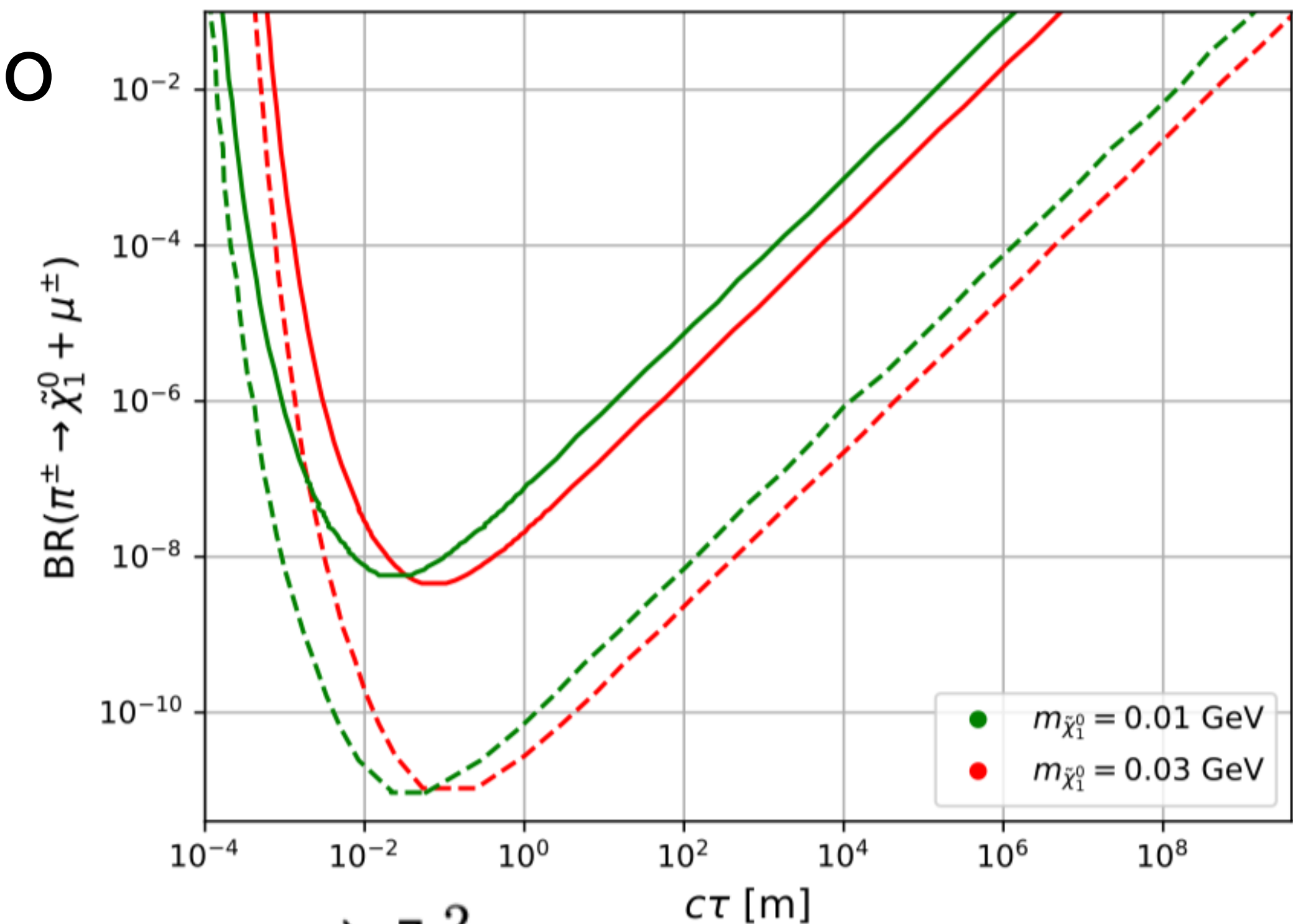


- Plus: scenarios with an even lighter neutralino

$$\pi^+ \rightarrow \ell^+ + \tilde{\chi}_1^0;$$

$$\tilde{\chi}_1^0 \rightarrow \gamma + \nu$$

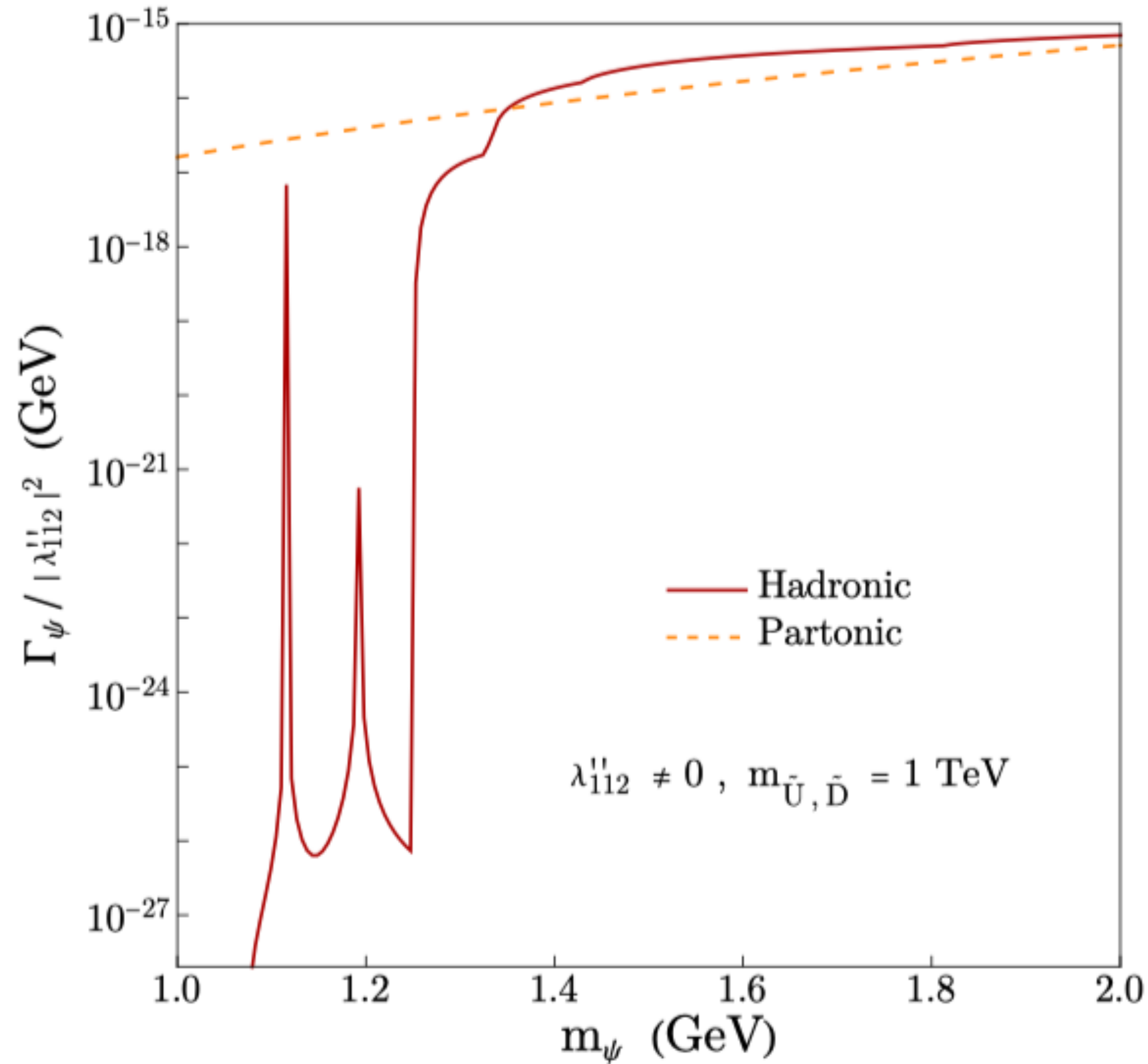
$$\Gamma(\tilde{\chi}_1^0 \rightarrow \gamma + \nu_i) = \frac{\lambda^2 \alpha^2 m_{\tilde{\chi}_1^0}^3}{512\pi^3 \cos^2 \theta_W} \left[ \sum_f \frac{e_f N_c m_f (4e_f + 1)}{m_{\tilde{f}}^2} \left( 1 + \log \frac{m_f^2}{m_{\tilde{f}}^2} \right)^2 \right]$$



# Neutralino Decays

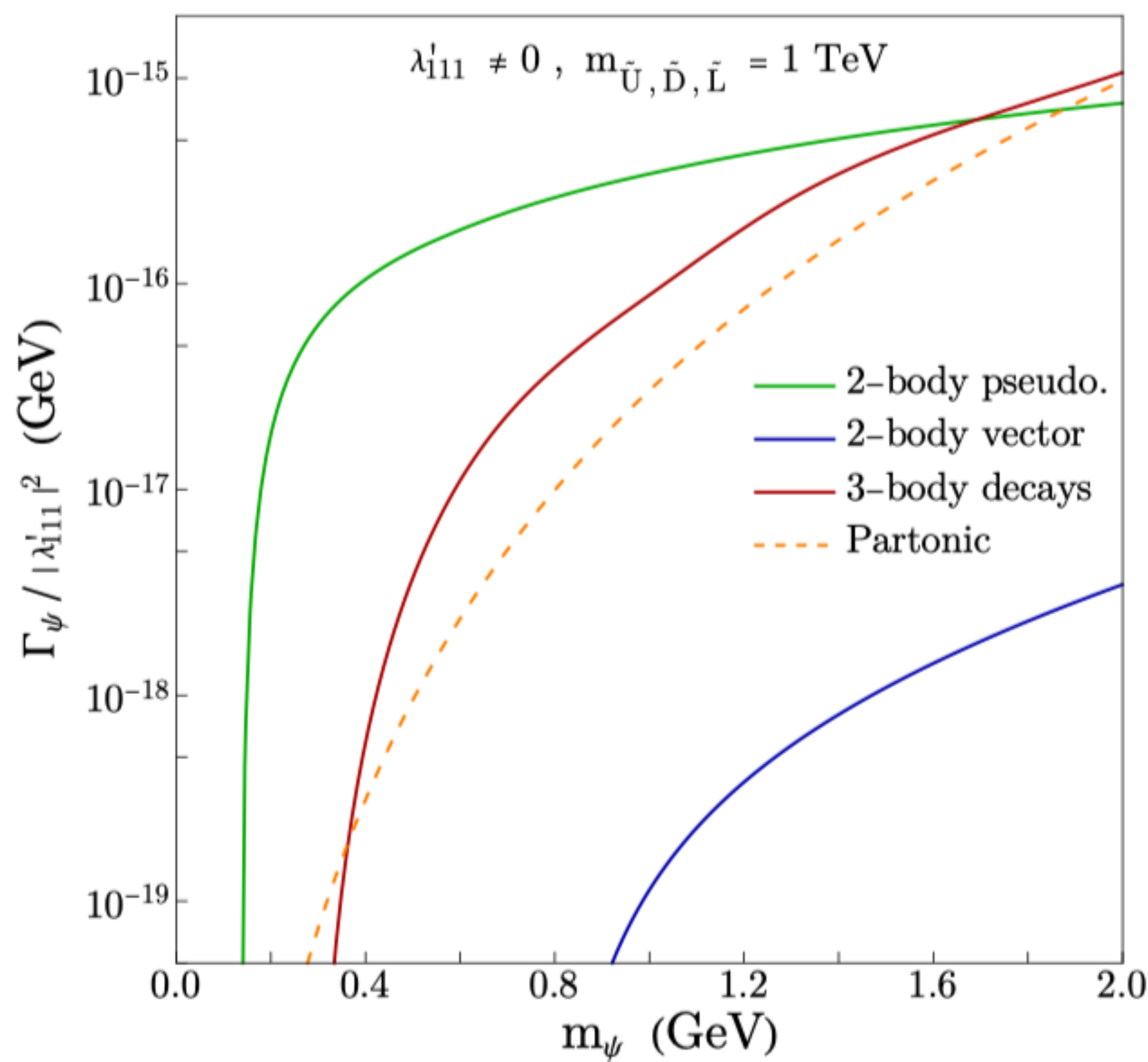
**UDD**

$\tilde{\chi}_1^0 \rightarrow p + M^-$



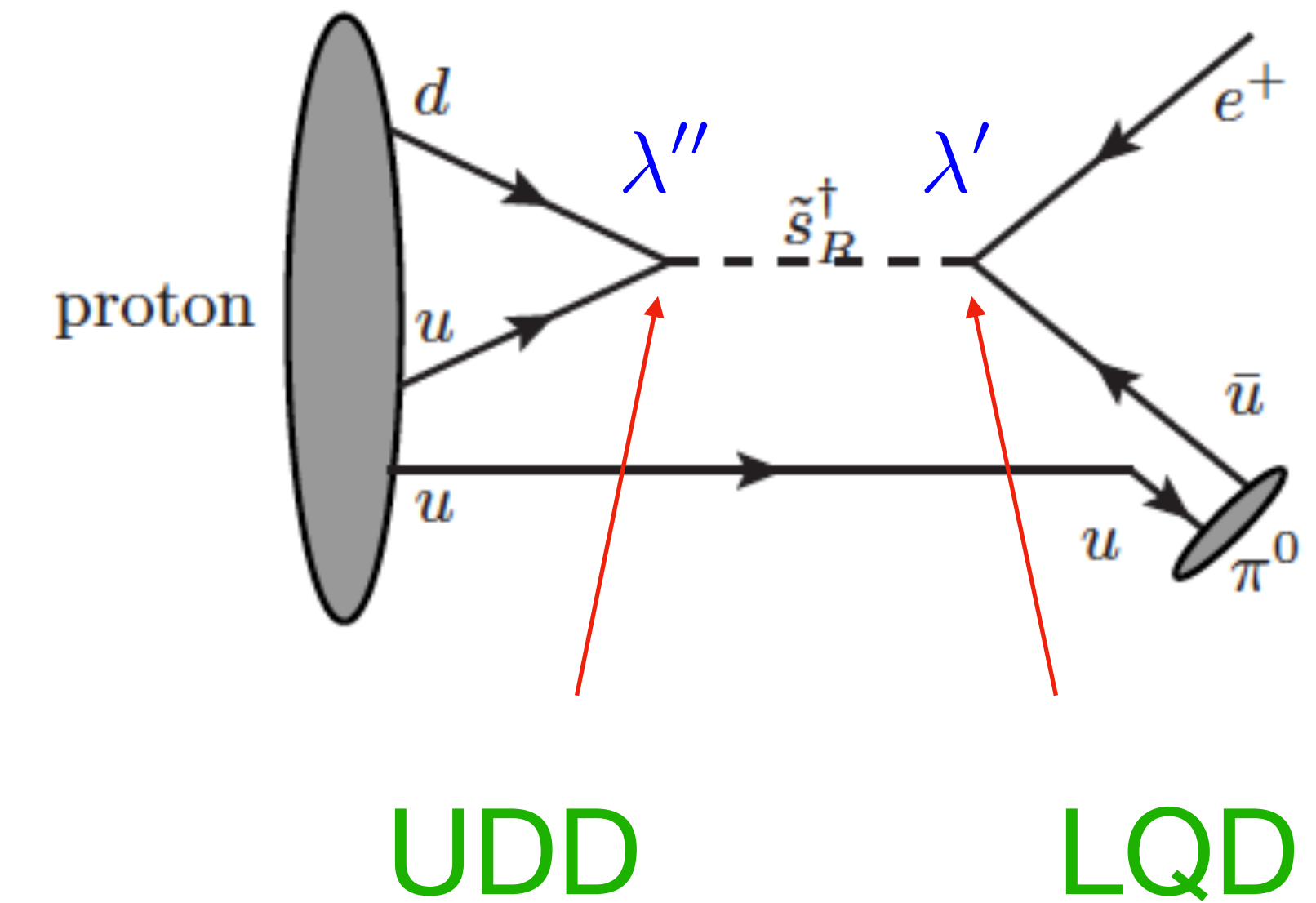
**LQD**

$\tilde{\chi}_1^0 \rightarrow M^\pm + \ell^\mp$



# Nucleon Decay

- Proton decays in R-parity Violating Supersymmetry



- Get strict bounds on the product:

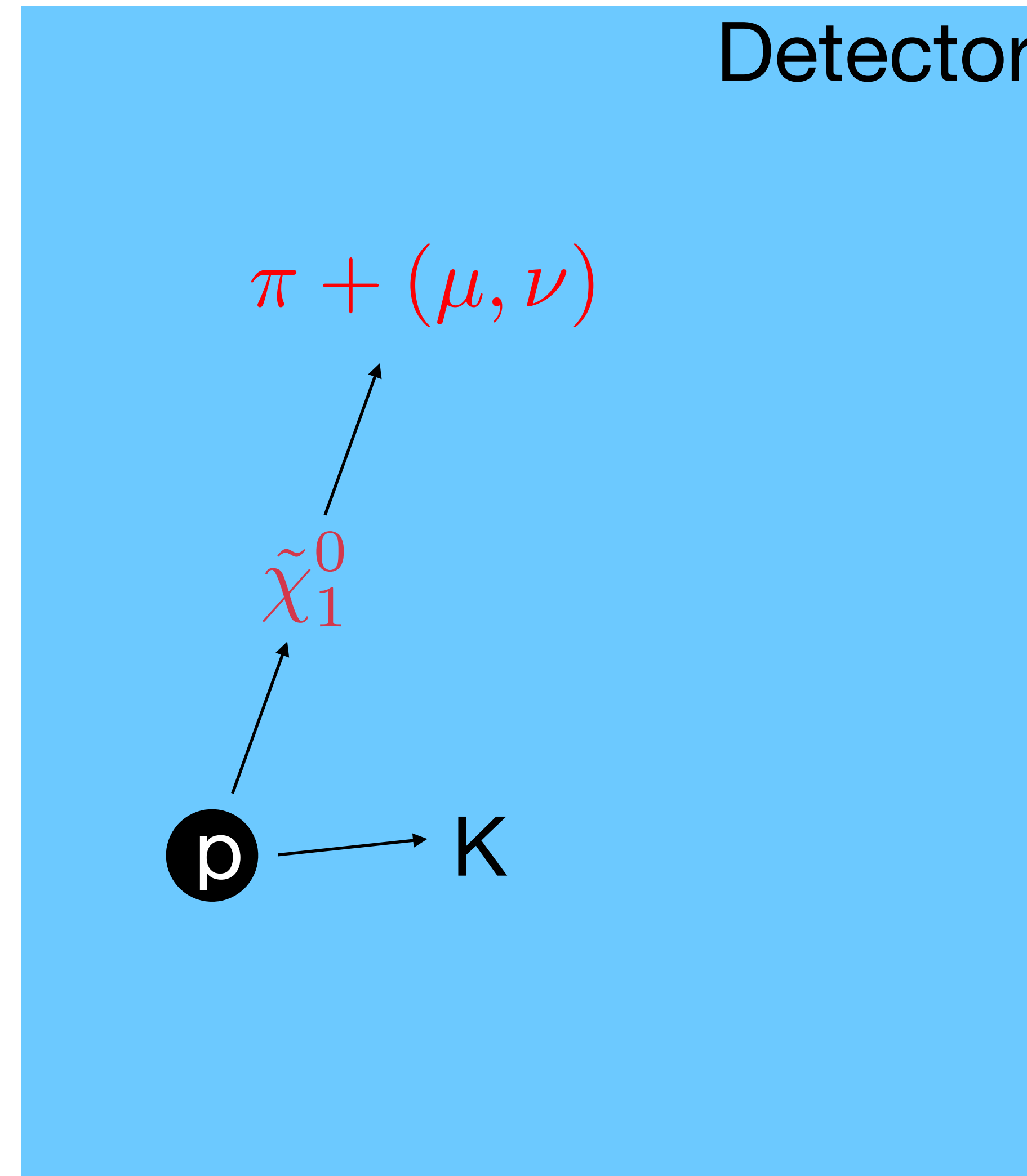
$$\frac{\lambda'' \cdot \lambda'}{M_{\text{SUSY}}^2}$$

- Reanalyzed these bounds, taking into account recent lattice results

- Nucleon decay in the R-parity violating MSSM

Nidal Chamoun, Florian Domingo, HKD; PRD. 104 (2021) 015020

# Proton Decay - Novel Decay Signature



- With: Florian Domingo, Apoorva Shah, Saurabh Nangia, Dominik Köhler: JHEP 05 (2024) 258

# Upcoming Detectors

	Super-K	Hyper-K	JUNO	DUNE
Location	Japan	Japan	China	USA
Geometry	Cylinder 42m height×39m diameter	Cylinder 60m height×74m diameter	Sphere 35.4m diameter	Cuboid (4 modules) 58.2m×14.0m×12.0m
Detector Material	Water	Water	LABs	Liquid Argon
Working Principle	Cherenkov	Cherenkov	Scintillation	Scintillation
Fiducial Mass	22.5kt	187kt	20kt	40kt
Approx. Start Year	-	2025	2024	2026

Table 1: Upcoming detectors for proton decay detection.

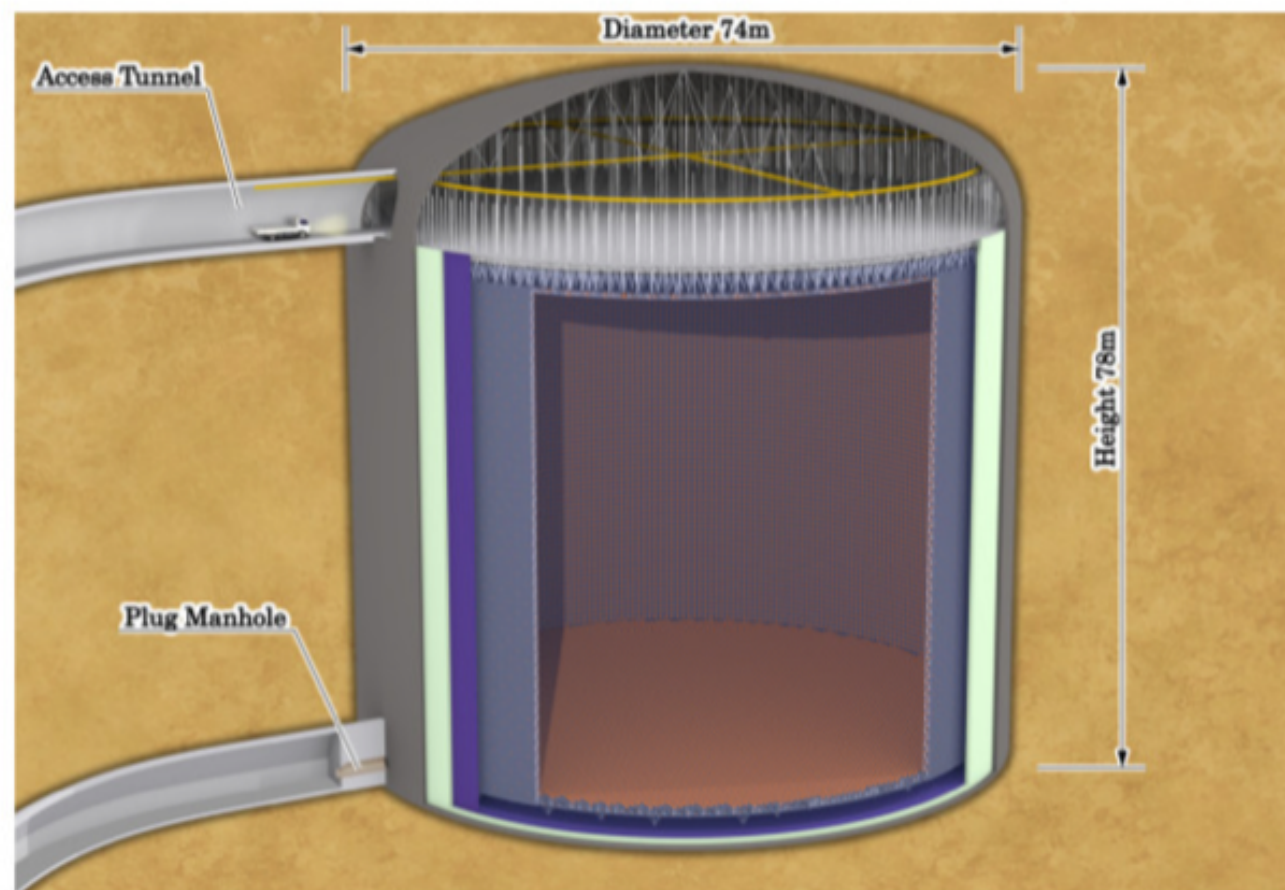


Figure 1: Hyper-K

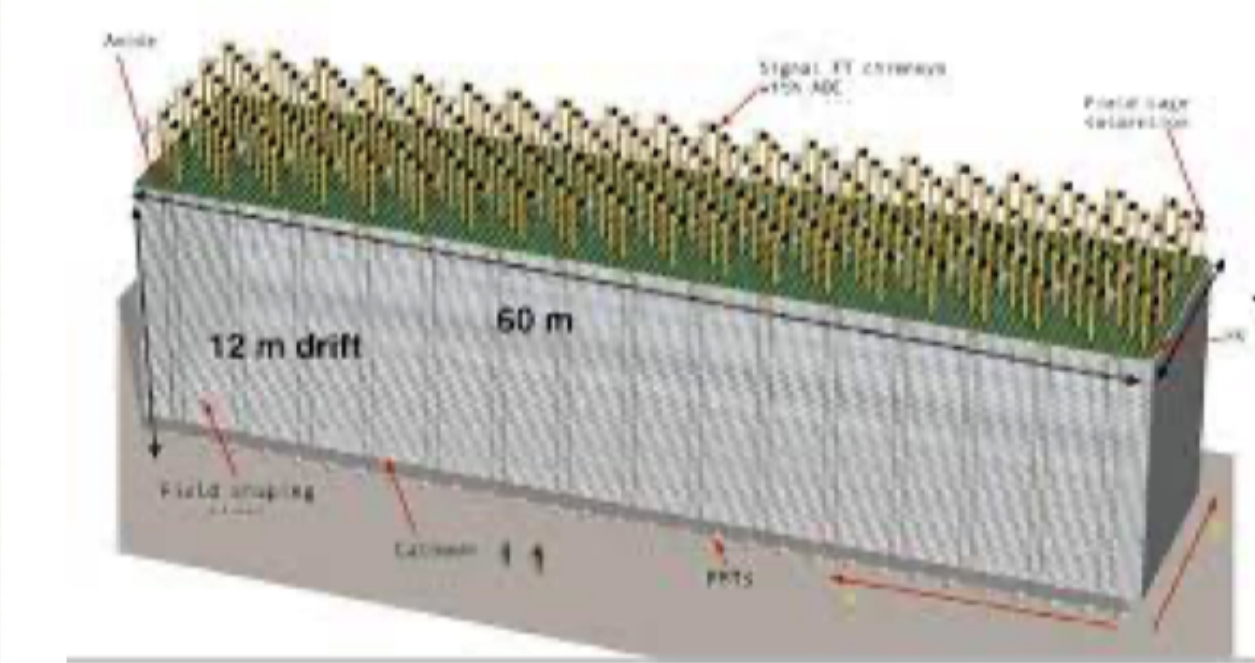


Figure 2: DUNE

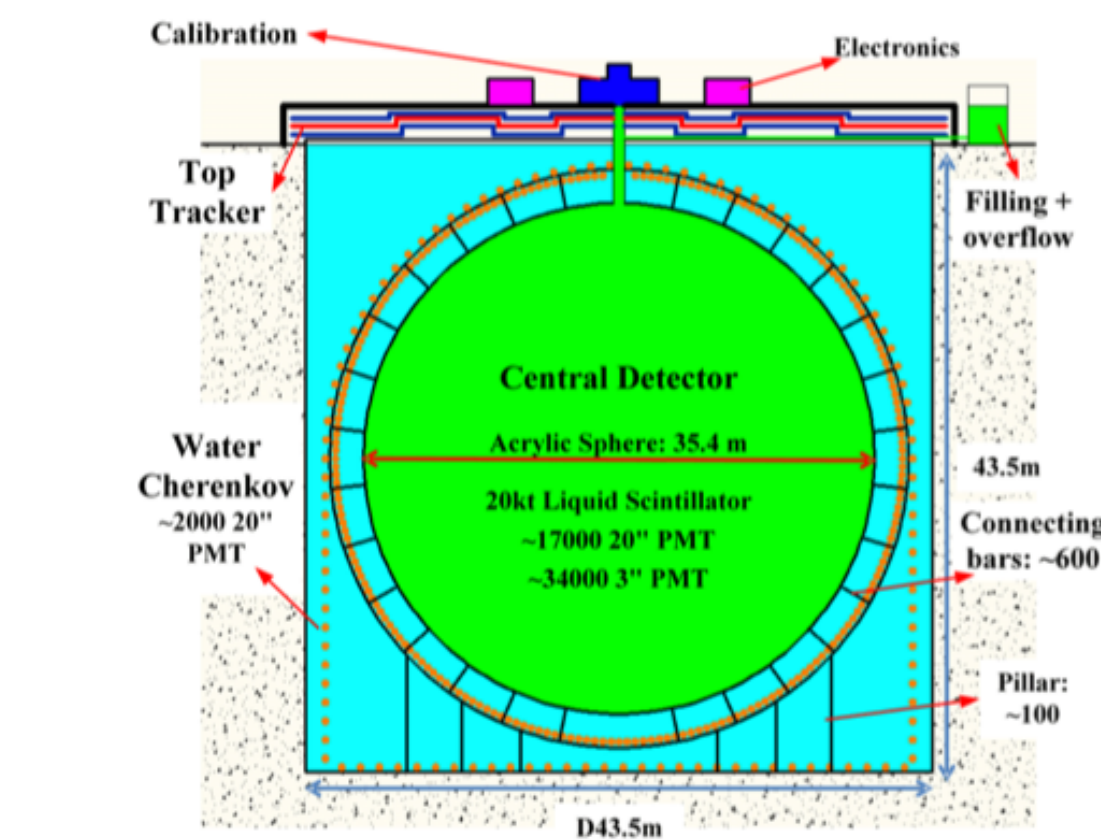
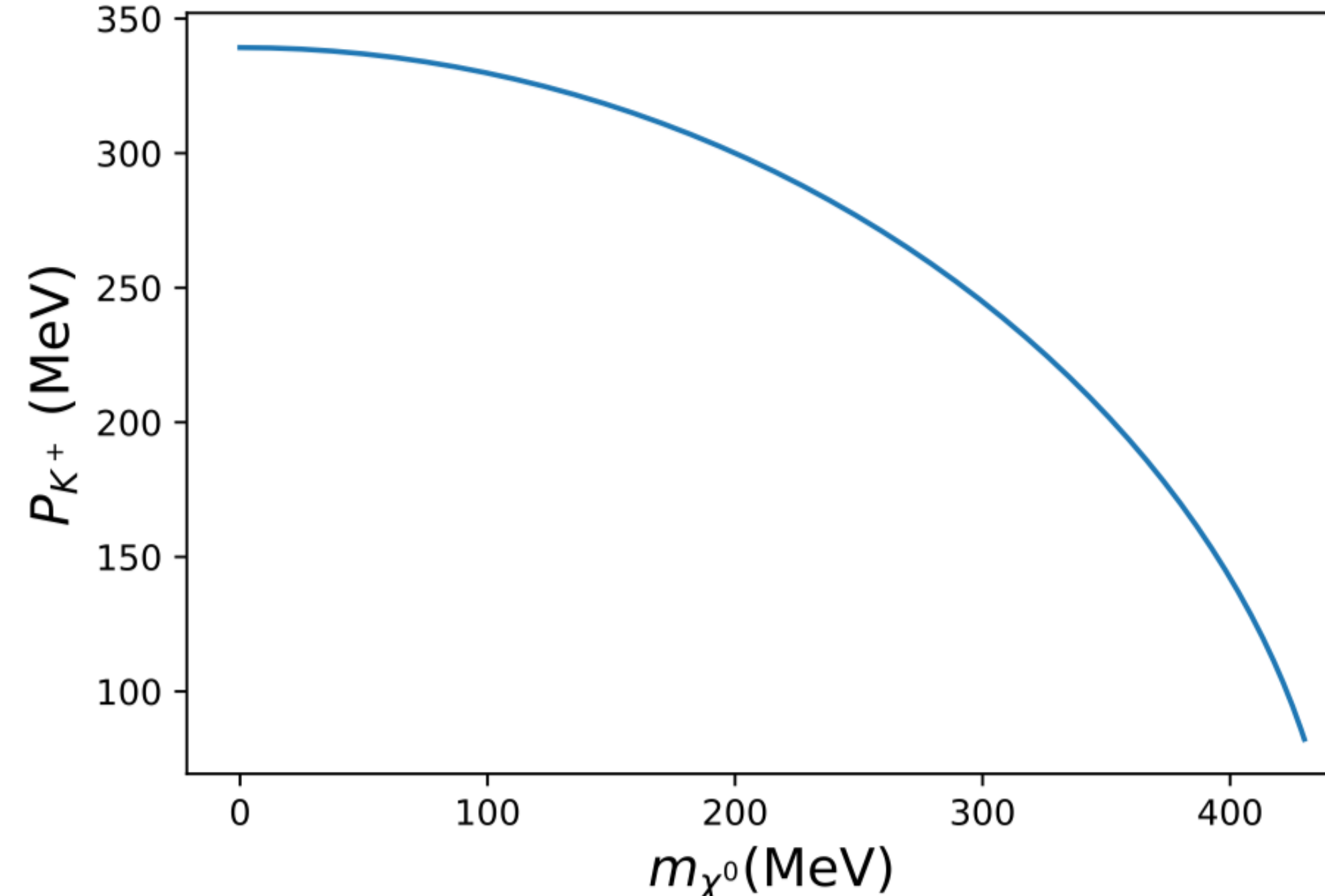


Figure 3: JUNO

includes  
CAS



**Figure 4:** Kaon momentum as a function of neutralino mass.

- The momentum of the Kaon is straightforward from kinematics.  
→ two-body decay
- For the neutrino,  $P_{K^+} \sim 330$  MeV
- $P_{K^+}$  is always lower than Cherenkov limit of water  
→ Hyper-K can only detect subsequent decays of Kaons.
- DUNE and JUNO can detect Kaons directly via scintillation.

- From Super-K limit, the number of proton decays/10 years is:  
 -Hyper-K:  $\sim 106$   
 -DUNE:  $\sim 18$   
 -JUNO:  $\sim 11$

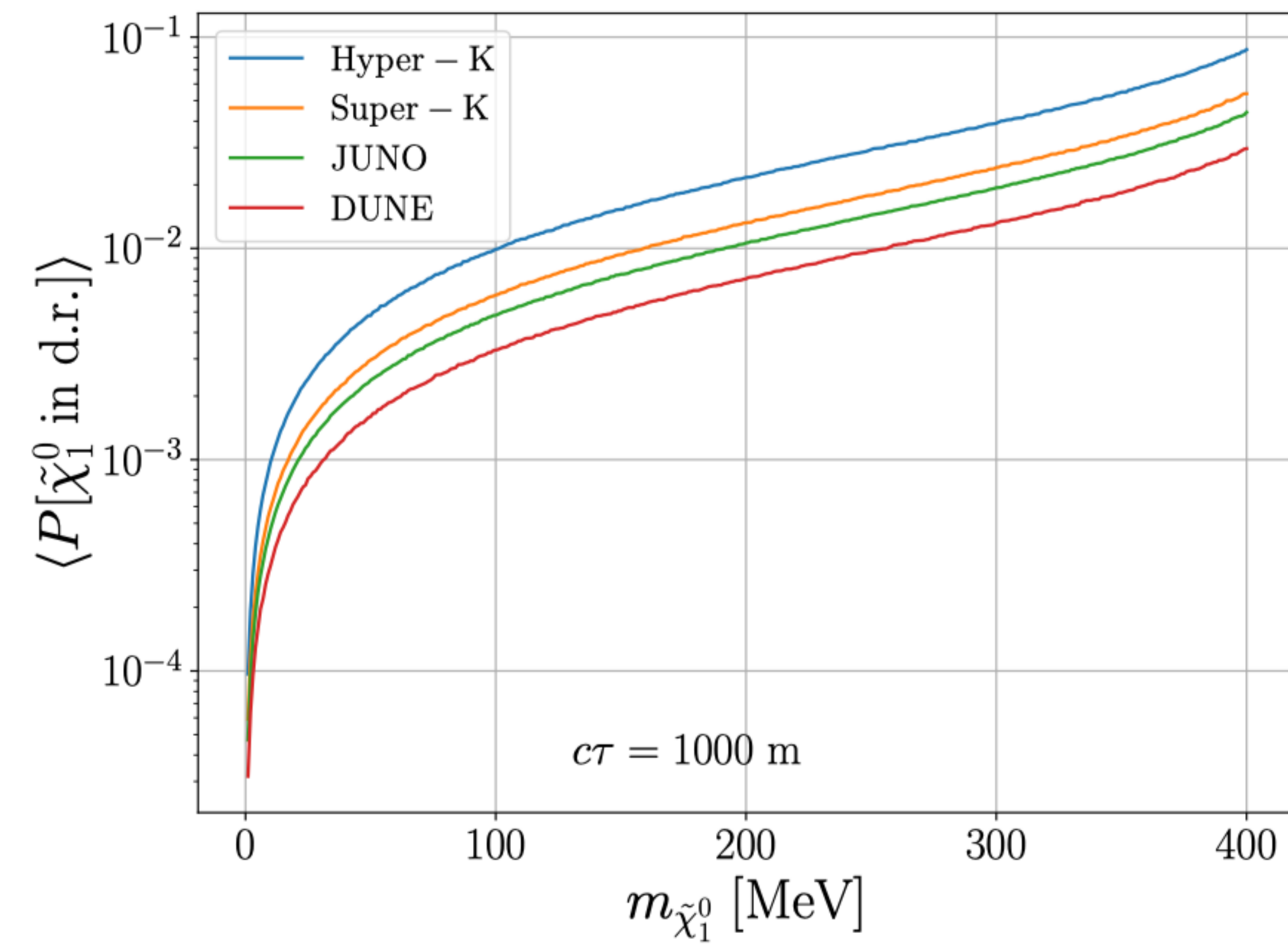
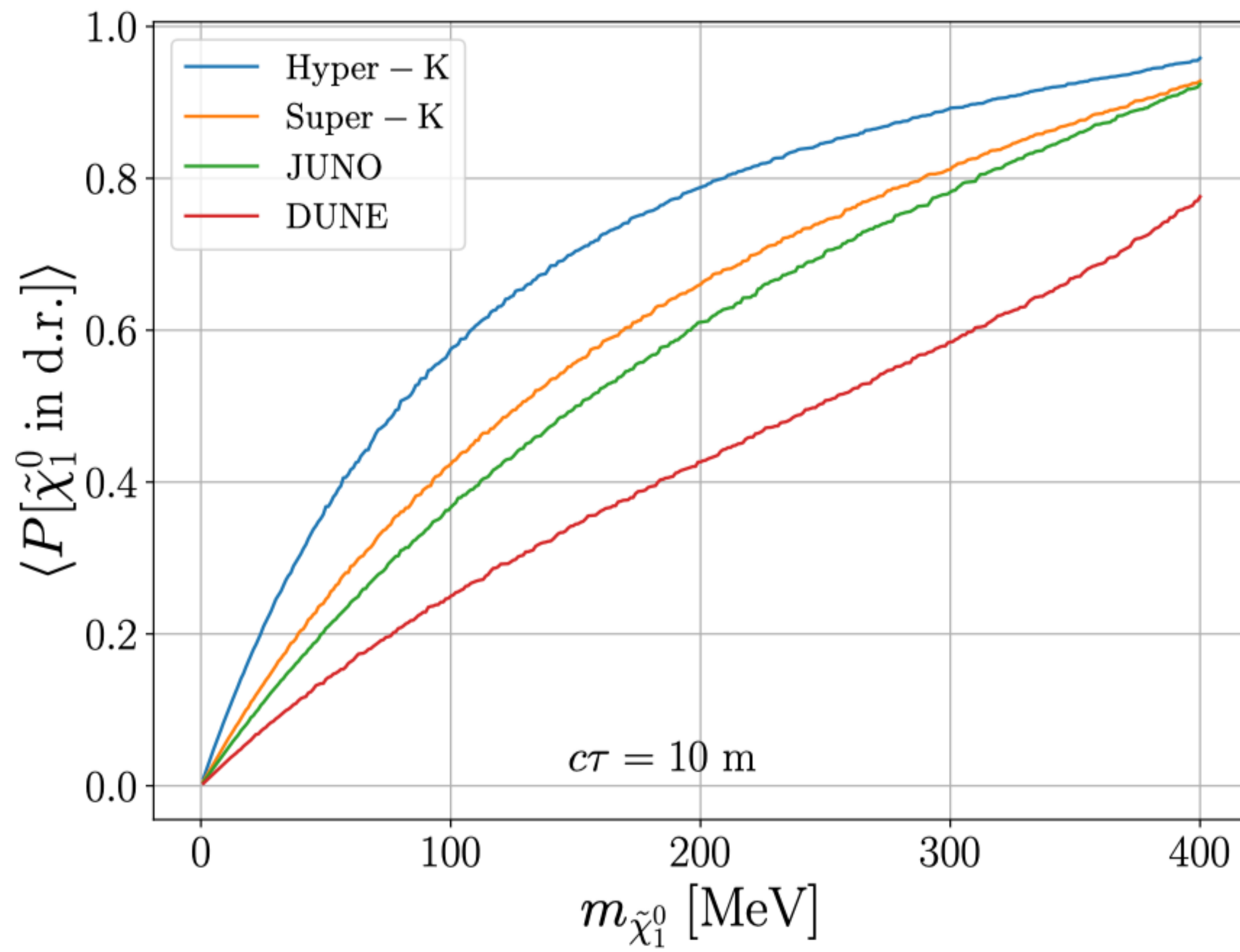


**Figure 4:** Average neutralino decay probabilities as a function of the neutralino mass for fixed neutralino decay length:  $c\tau = 10 \text{ m}$  (left) and  $c\tau = 1000 \text{ m}$  (right). These plots have been generated with a sample size  $N_{\tilde{\chi}_1^0}^{\text{MC}} = 10,000$ .

# Proton Decay Benchmarks

Scenario	$m_{\tilde{\chi}_1^0}$	Proton Decay	$\tilde{\chi}_1^0$ Decay ( $\lambda_{ijk}^D$ )	Product Bound	Min. $c\tau_{\tilde{\chi}_1^0}$
<b>B1</b>	0 – 400 MeV	$\lambda''_{121} < 5 \times 10^{-7} \left( \frac{m_{\tilde{q}}}{\tilde{\Lambda}\text{TeV}} \right)^{5/2}$	–	–	$\infty$
<b>B2</b>	0 – 400 MeV	$\lambda''_{121} < 5 \times 10^{-7} \left( \frac{m_{\tilde{q}}}{\tilde{\Lambda}\text{TeV}} \right)^{5/2}$	$\lambda'_{333} < 1.04$	$\lambda'_{333} \lambda''_{121} < 10^{-9}$	$\sim 1600$ m
<b>B3</b>	0 – 400 MeV	$\lambda''_{121} < 5 \times 10^{-7} \left( \frac{m_{\tilde{q}}}{\tilde{\Lambda}\text{TeV}} \right)^{5/2}$	$\lambda_{233} < 0.7 \left( \frac{m_{\tilde{\tau}_R}}{1\text{TeV}} \right)$	$\lambda_{233} \lambda''_{121} < 10^{-21}$	$\sim 180$ m
<b>B4</b>	150 – 400 MeV	$\lambda''_{121} < 5 \times 10^{-7} \left( \frac{m_{\tilde{q}}}{\tilde{\Lambda}\text{TeV}} \right)^{5/2}$	$\lambda'_{211} < 0.59 \left( \frac{m_{\tilde{d}_R}}{1\text{TeV}} \right)$	$\lambda'_{211} \lambda''_{121} < 6 \times 10^{-25}$	$\sim 11$ m
<b>B5</b>	150 – 400 MeV	$\lambda''_{121} < 5 \times 10^{-7} \left( \frac{m_{\tilde{q}}}{\tilde{\Lambda}\text{TeV}} \right)^{5/2}$	$\lambda'_{311} < 1.12$	$\lambda'_{311} \lambda''_{121} < 4 \times 10^{-24}$	$\sim 8$ m

**B1:** no  $\tilde{\chi}_1^0$ -decay

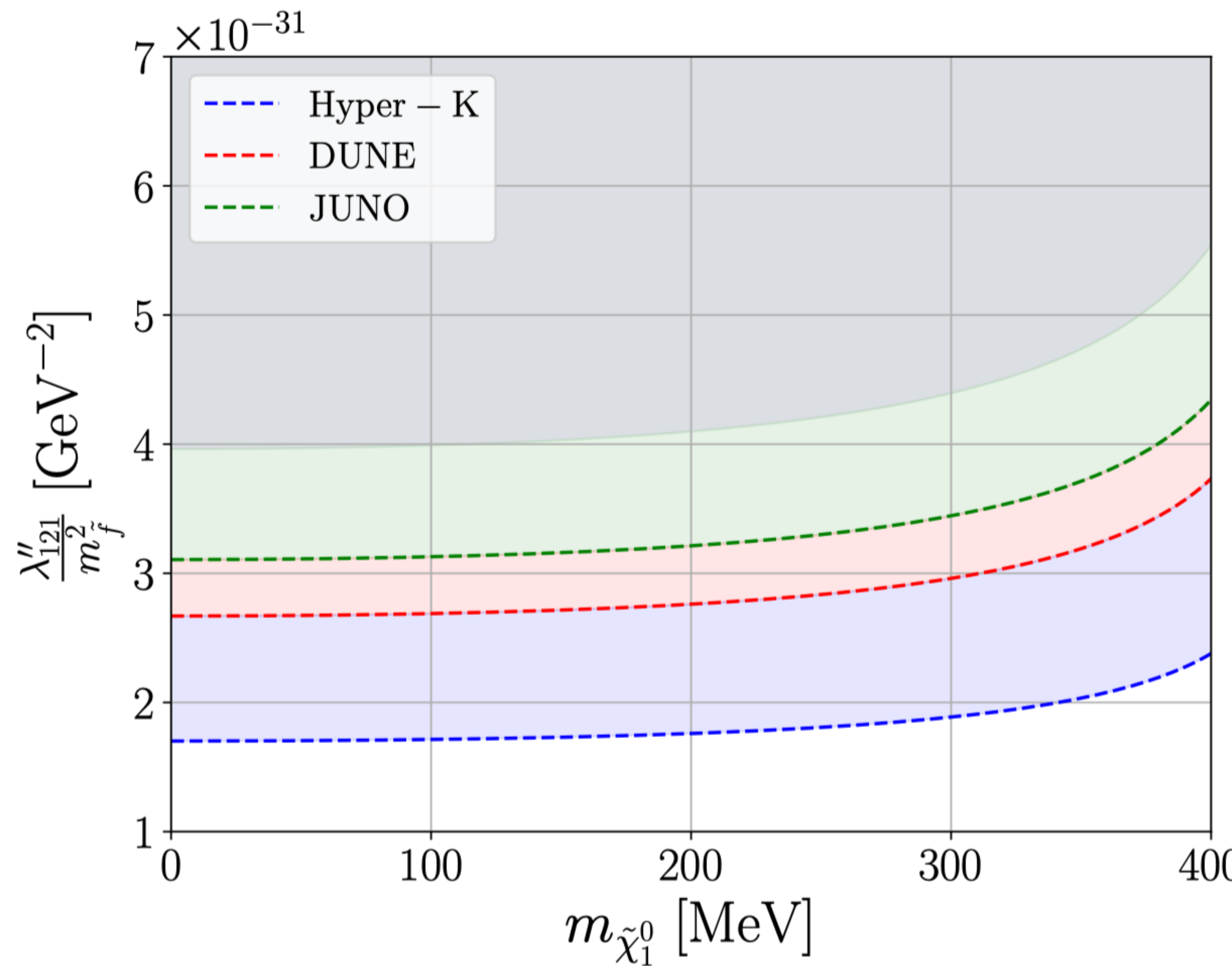
**B2:**  $\tilde{\chi}_1^0 \rightarrow \gamma + \nu$

**B3:**  $\tilde{\chi}_1^0 \rightarrow \gamma + \nu$

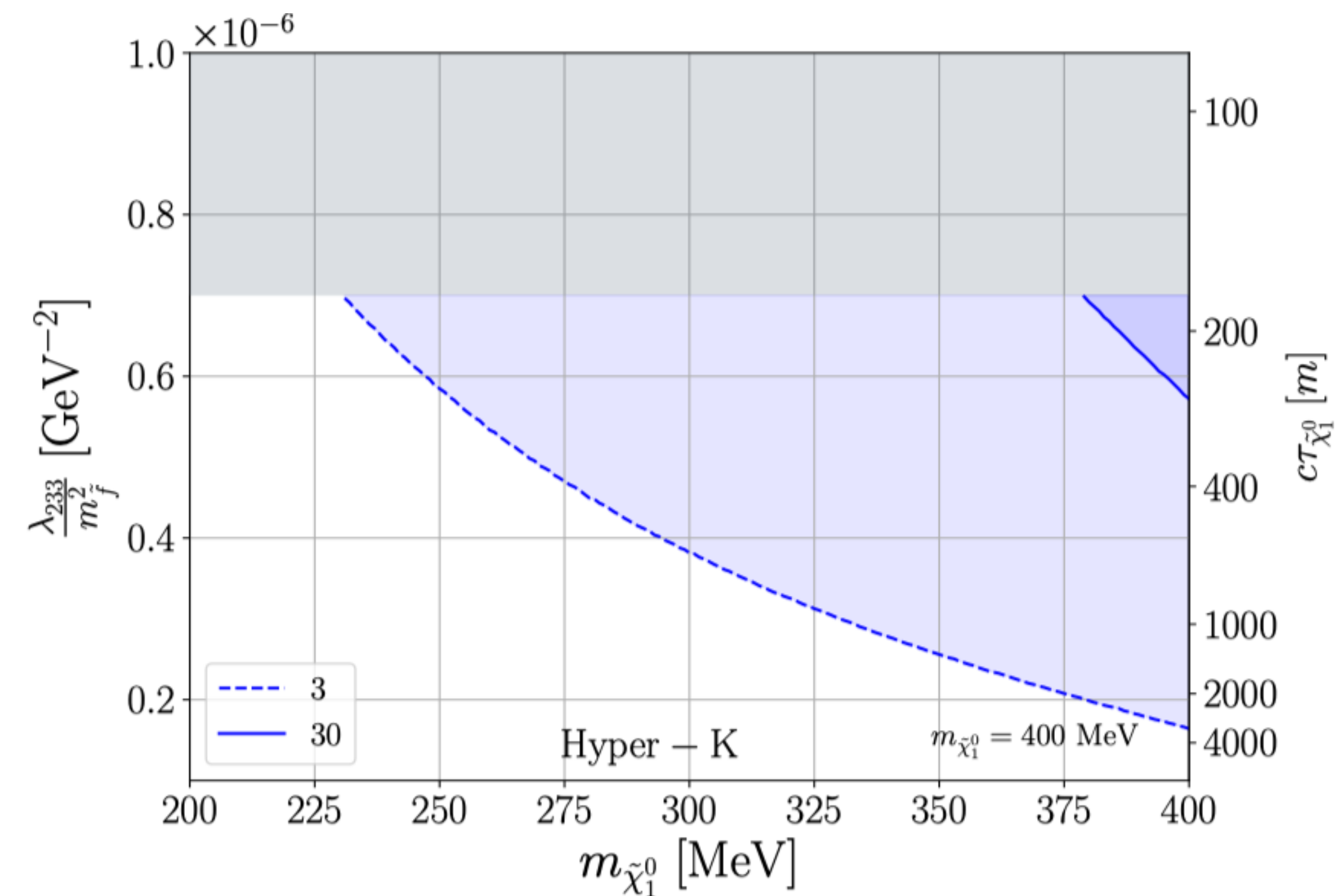
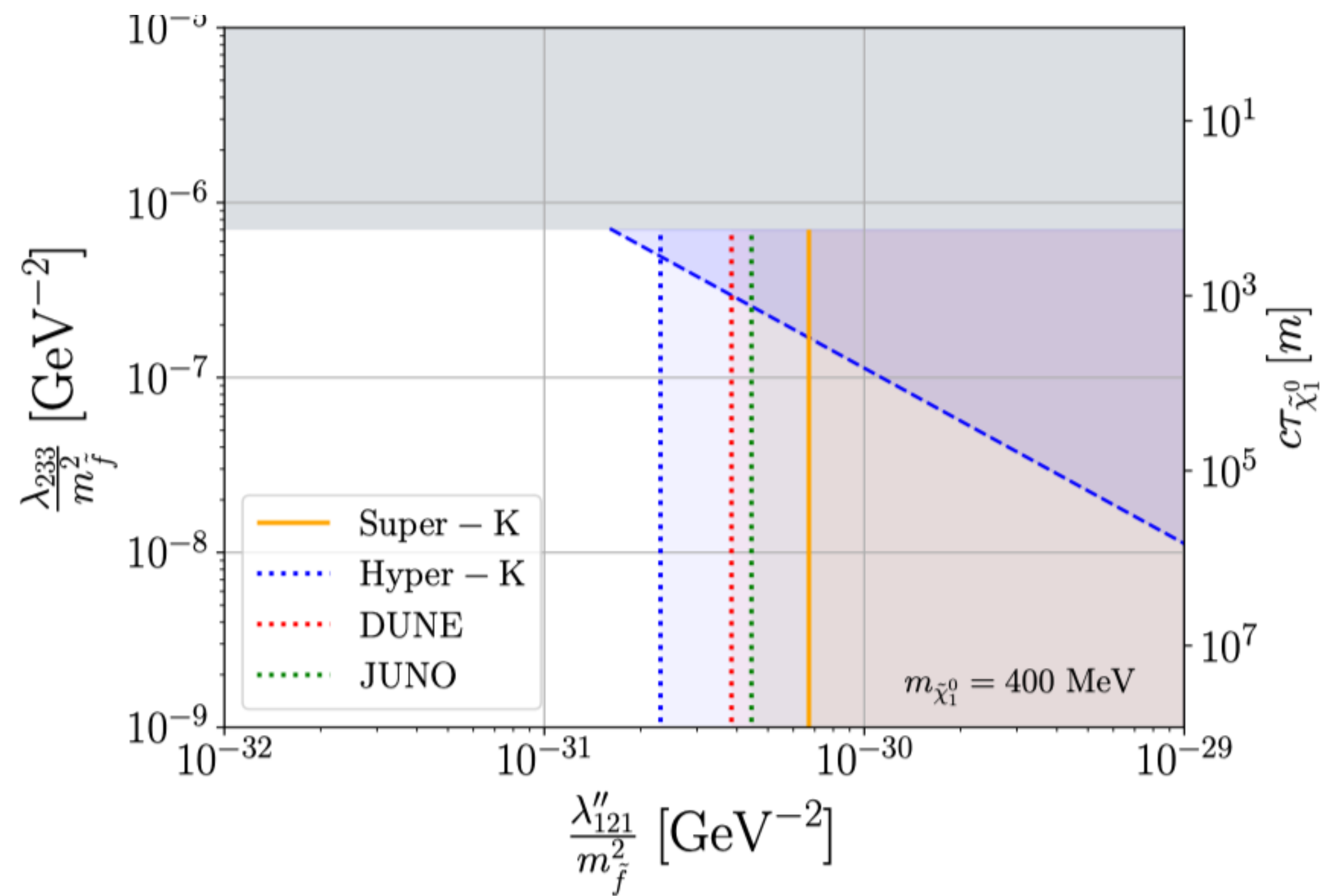
**B4:**  $\tilde{\chi}_1^0 \rightarrow (\pi^\pm + \mu^\mp, \pi^0 + \nu_\mu)$        $m_{\pi^-} + m_\mu \leq \tilde{\chi}_1^0 < m_p - m_{K^+}$

**B5:**  $\tilde{\chi}_1^0 \rightarrow \pi^0 + \nu_\mu$        $m_{\pi^0} \leq \tilde{\chi}_1^0 < m_p - m_{K^+}$

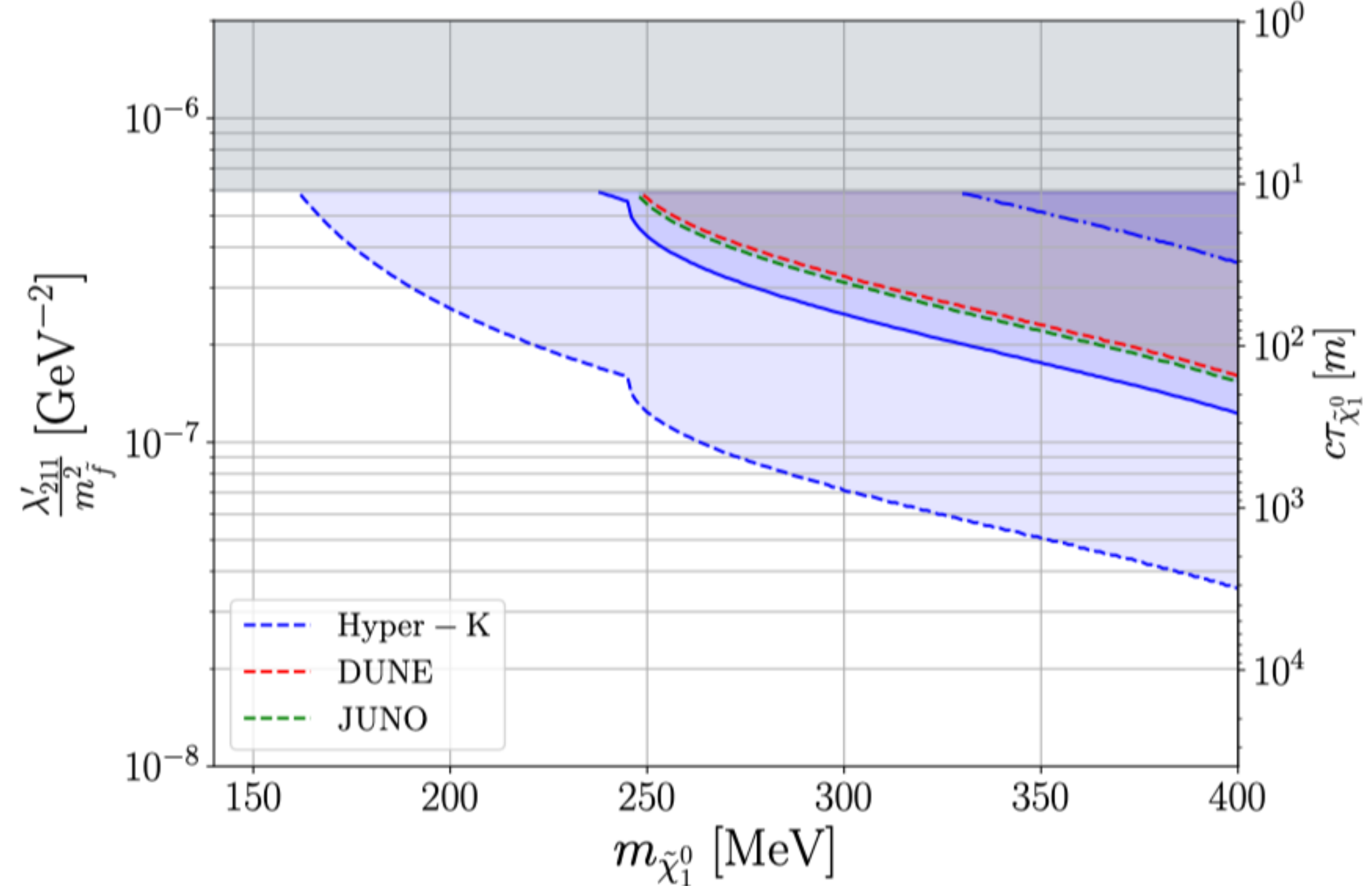
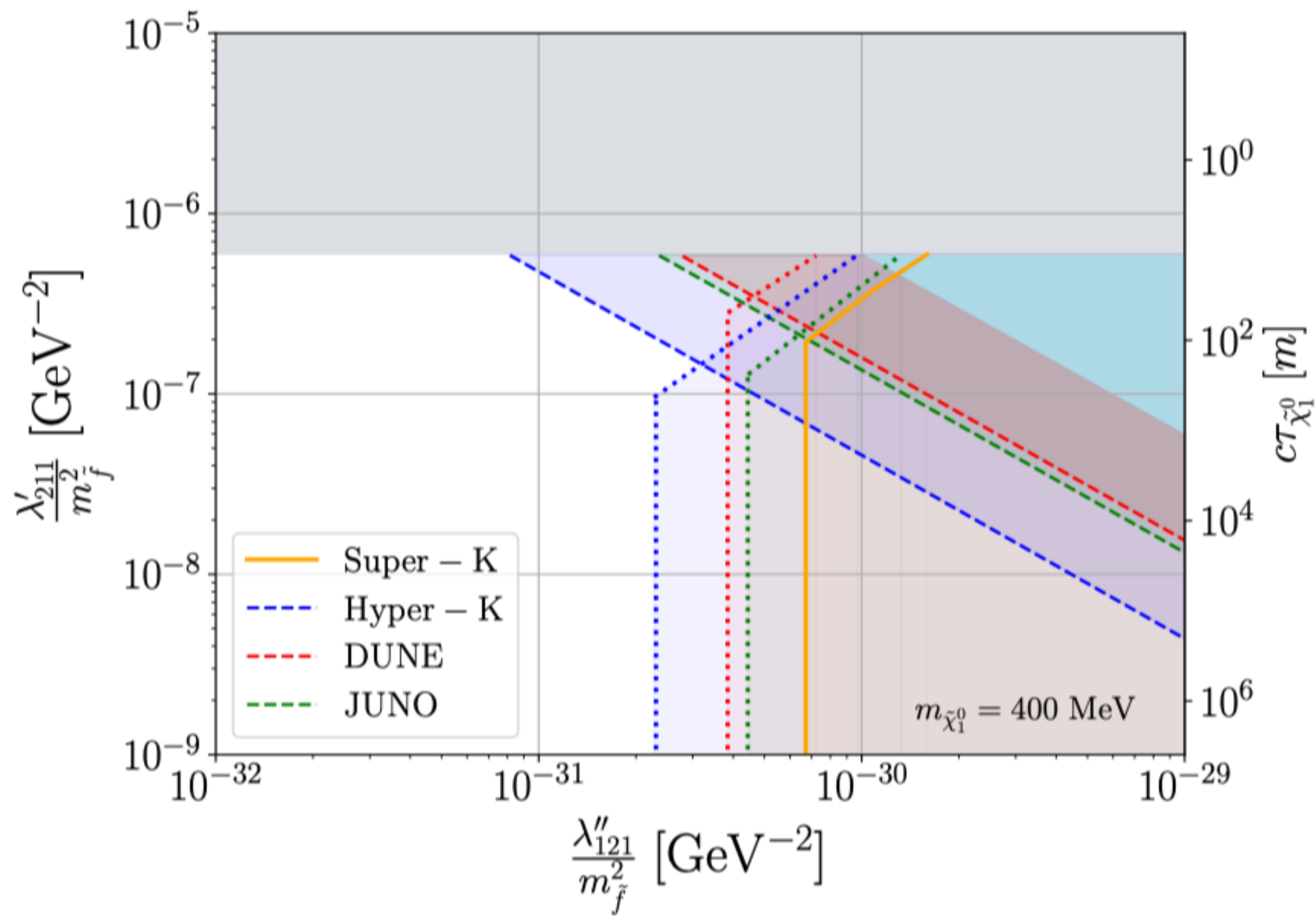
## B1



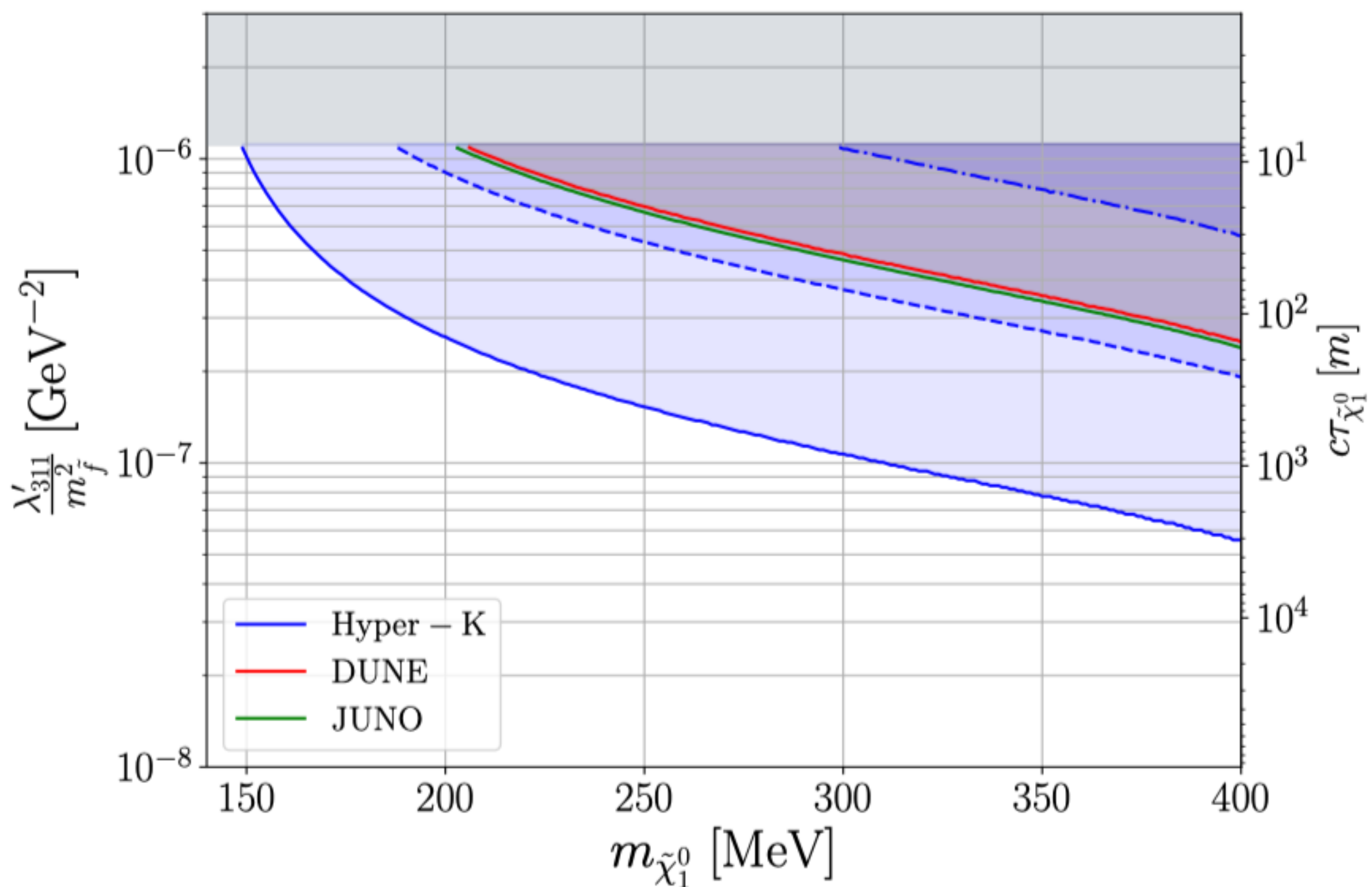
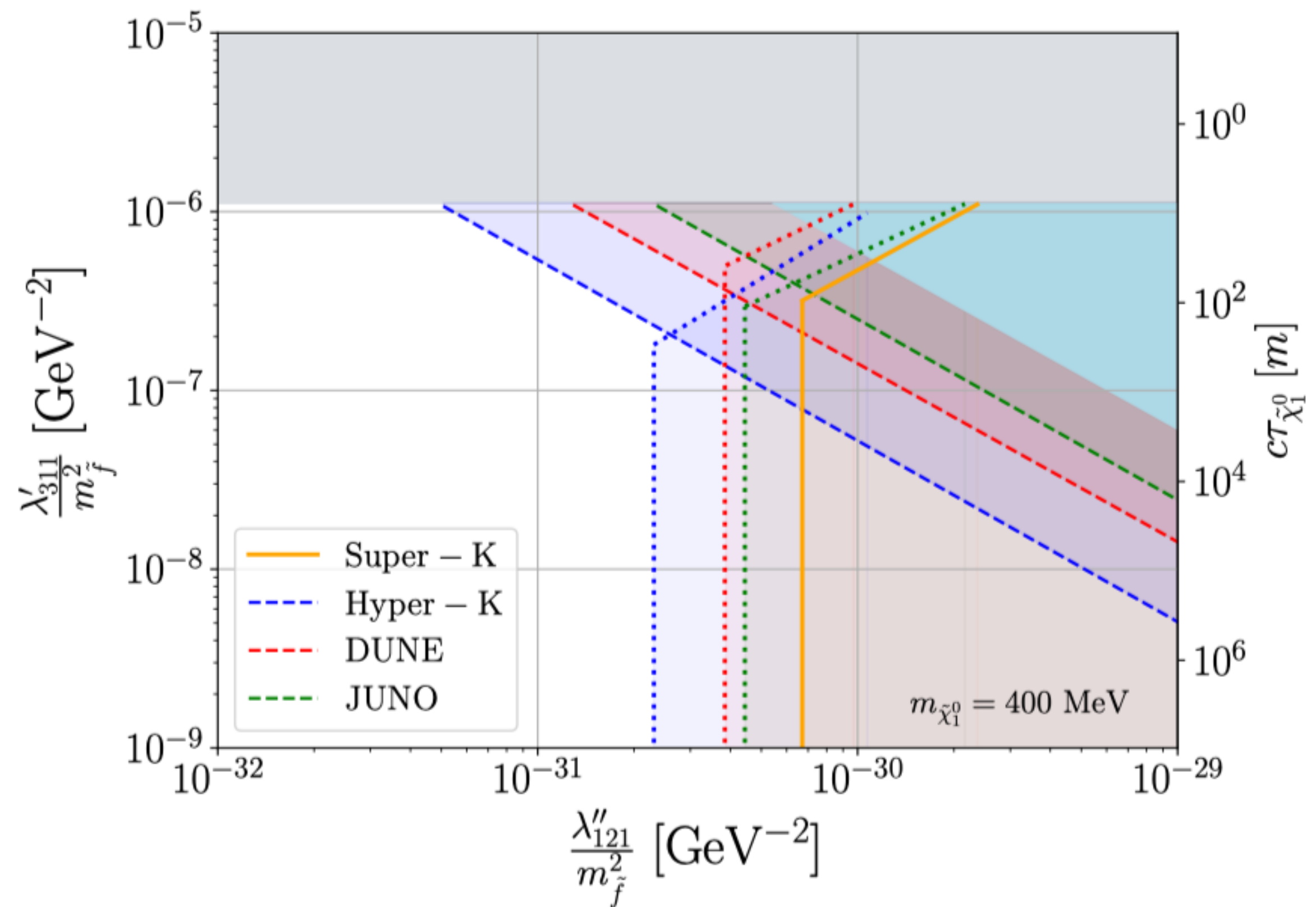
**Figure 5:** Sensitivity reach for the single coupling scenario of benchmark **B1**. The reinterpreted bound from Super-K is shown in gray. The bound from Table 2 lies above the scale of the plot. The results for Hyper-K, DUNE, and JUNO are for a run-time of 10 years.

**B3** $\tilde{\chi}_1^0 \rightarrow \gamma + \nu$  $c\tau_{\tilde{\chi}_1^0} \sim 180 \text{ m}$ 

**Figure 7:** Sensitivity reach/Super-K limit for benchmark **B3**. The existing single-bounds from Table 2 are shown in gray while the product-bound is shown in blue (all with  $m_{\tilde{f}} = 1$  TeV). *Top Left:* As in left plot of Fig. 6 but for benchmark **B3**. *Top Right:* Zoomed-out version of the top-left plot. *Bottom:* As in right plot of Fig. 5 but for benchmark **B3**. The dashed and solid lines correspond to 3- and 30-event isocurves, respectively.

**B4** $\tilde{\chi}_1^0 \rightarrow (\pi^\pm + \mu^\mp, \pi^0 + \nu_\mu)$  $c\tau_{\tilde{\chi}_1^0} \sim 11 \text{ m}$ 

**Figure 8:** Sensitivity reach/**Super-K** limit for benchmark **B4**. The existing single-bound on  $\lambda'_{211}$  from Table 2 is shown in gray, the product-bound is in light blue (both with  $m_{\tilde{f}} = 1 \text{ TeV}$ ), while the bound on  $\lambda''_{121}$  lies outside the scale of the plot. *Left:* As in left plot of Fig. 6 but for benchmark **B4**. *Right:* As in right plot of Fig. 5 but for benchmark **B4**. The dashed, solid, and dot-dashed lines correspond to 3-, 30- and 90-event isocurves, respectively. An interesting thing to note is the kink in sensitivity in the right figure around  $m_{\tilde{\chi}_1^0} \sim 240 \text{ MeV}$ , which is due to the modes  $\tilde{\chi}_1^0 \rightarrow \pi^\pm + \mu^\mp$  being kinematically allowed, thus increasing the total decay width.

**B4**
 $\tilde{\chi}_1^0 \rightarrow (\pi^\pm + \mu^\mp, \pi^0 + \nu_\mu)$ 
 $c\tau_{\tilde{\chi}_1^0} \sim 8 \text{ m}$ 


**Figure 9:** Sensitivity reach/Super-K limit for benchmark **B5**. The existing single-bound on  $\lambda'_{311}$  from Table 2 is shown in gray, the product-bound is in light blue (both with  $m_{\tilde{f}} = 1 \text{ TeV}$ ), while the bound on  $\lambda''_{121}$  lies outside the scale of the plot. *Left:* As in left plot of Fig. 6 but for benchmark **B5**. *Right:* As in right plot of Fig. 5 but for benchmark **B5**. The dashed, solid, and dot-dashed lines correspond to 3-, 30- and 90-event isocurves,

# New Show: Far From Home



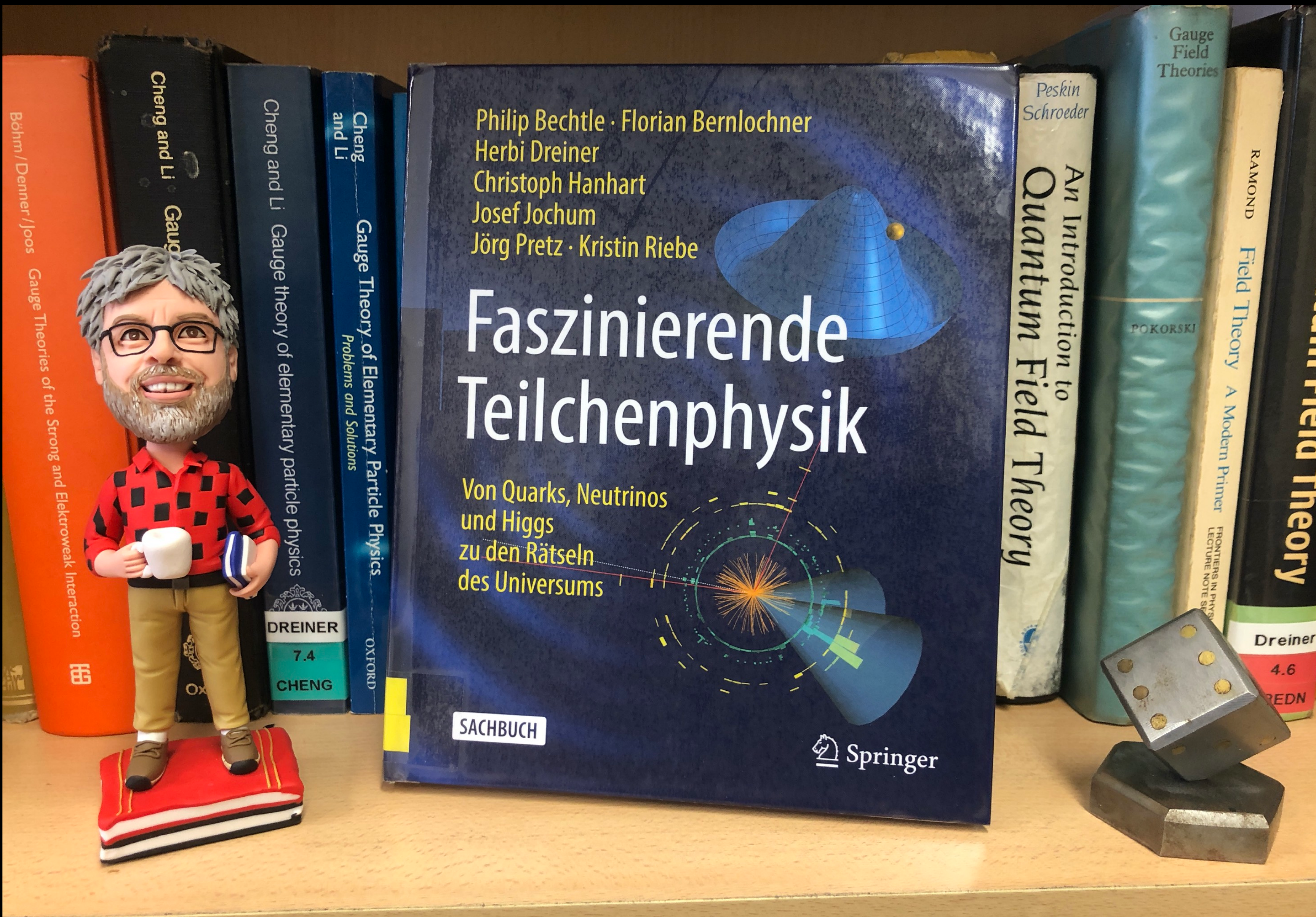
Bonn Sept. 2023

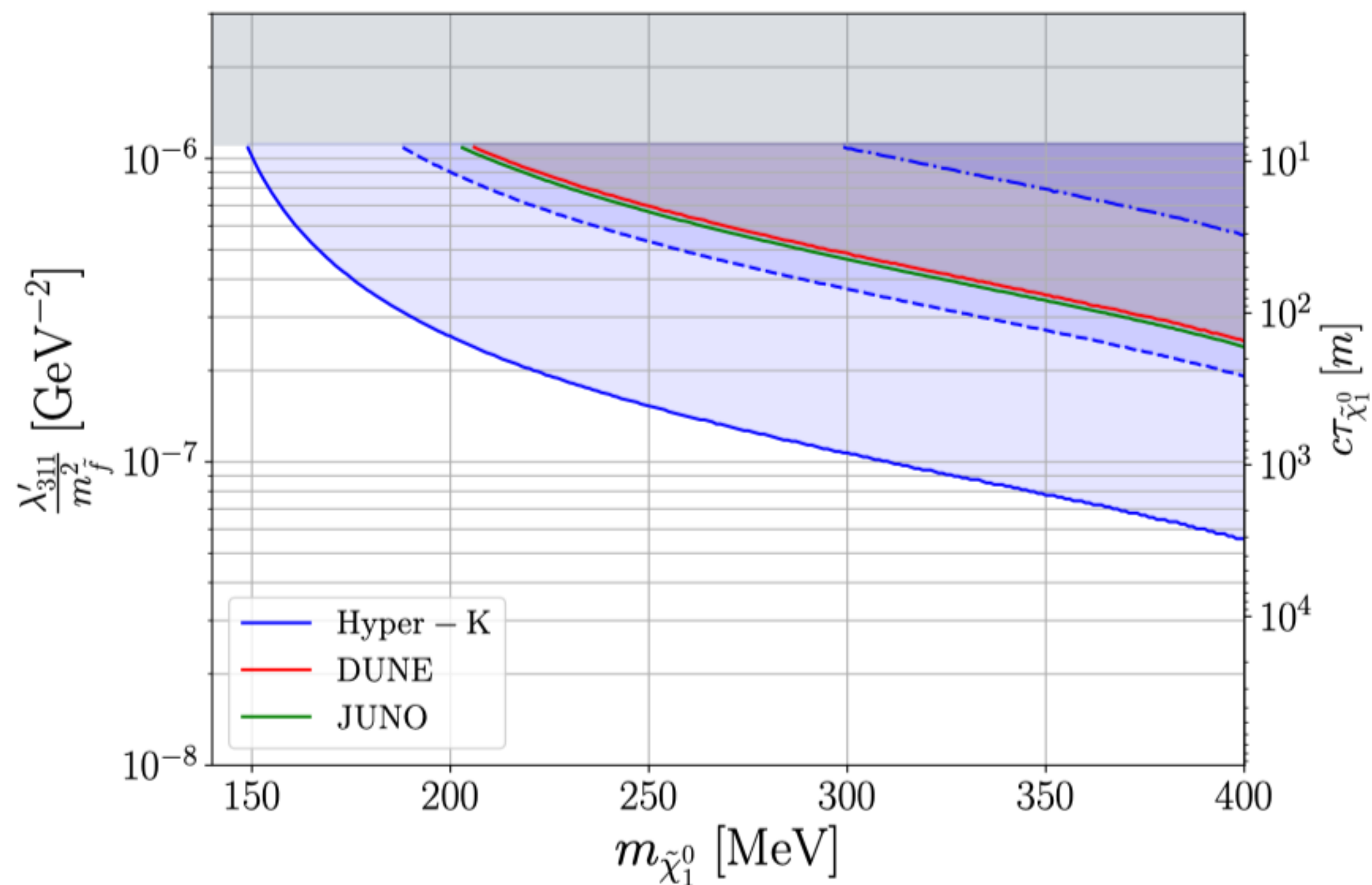
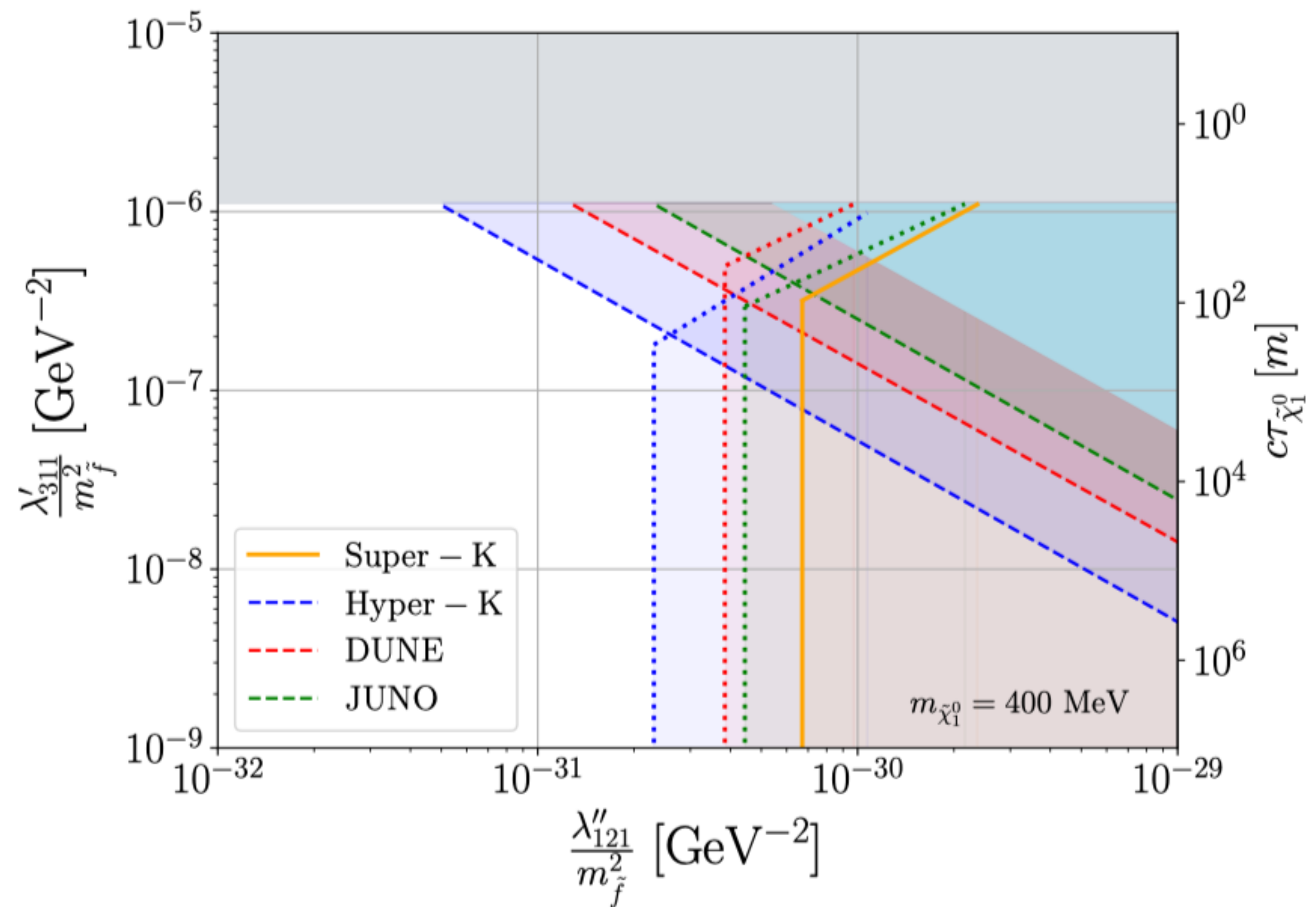
# PLANETAMOS



Tübingen (3/2023)

# Fascinating Particle Physics: a Popular Book Project



**B4**
 $\tilde{\chi}_1^0 \rightarrow (\pi^\pm + \mu^\mp, \pi^0 + \nu_\mu)$ 
 $c\tau_{\tilde{\chi}_1^0} \sim 8 \text{ m}$ 


**Figure 9:** Sensitivity reach/Super-K limit for benchmark **B5**. The existing single-bound on  $\lambda'_{311}$  from Table 2 is shown in gray, the product-bound is in light blue (both with  $m_{\tilde{f}} = 1 \text{ TeV}$ ), while the bound on  $\lambda''_{121}$  lies outside the scale of the plot. *Left:* As in left plot of Fig. 6 but for benchmark **B5**. *Right:* As in right plot of Fig. 5 but for benchmark **B5**. The dashed, solid, and dot-dashed lines correspond to 3-, 30- and 90-event isocurves,

# Back-Up Slides

# Decay of Light Neutralinos (MeV - range)

Systematic study of light neutralino (Bino) decays

Decays of a bino-like particle in the low-mass regime

Florain Domingo, HKD; arXiv:2205.08141 [hep-ph] (50p)

- General superpotential

$$W_{\text{RpV}} = \mu_i \hat{H}_u \cdot \hat{L}_i + \frac{1}{2} \lambda_{ijk} \hat{L}_i \cdot \hat{L}_j (\hat{E}^c)_k + \lambda'_{ijk} \hat{L}_i \cdot \hat{Q}_{j\alpha} (\hat{D}^c)_k^\alpha + \frac{1}{2} \lambda''_{ijk} \varepsilon_{\alpha\beta\gamma} (\hat{U}^c)_i^\alpha (\hat{D}^c)_j^\beta (\hat{D}^c)_k^\gamma,$$



neutralinos and  
neutrinos mix

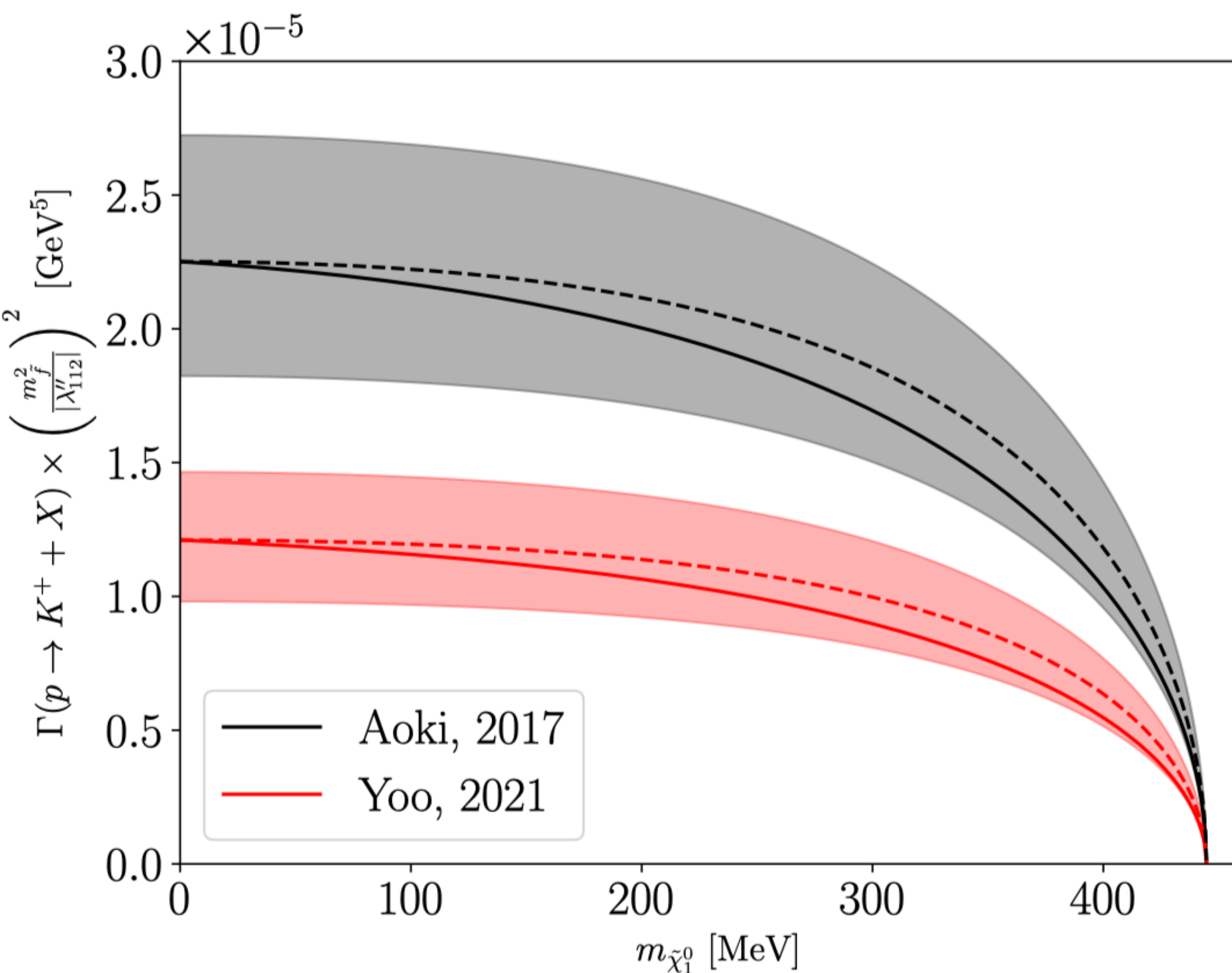


**Figure 2:** Proton decay width normalised to  $|\lambda''_{112}|^2/m_{\tilde{f}}^4$ , where  $m_{\tilde{f}}$  represents a universal value for the squark masses. Two different lattice evaluations are used for the numerical values of the form factors: from Aoki, 2017 [84] and Yoo, 2021 [85]. The dashed line represents the case where lattice form-factors at  $q^2 = 0$  are used, whatever the neutralino mass, while the solid lines represent results with form factors determined according to chiral perturbation theory [83]. The bands around the dashed lines denote the approximate error in the lattice calculation of the form factors.

- Derive effective field theory
- dimension-6 operators

- electromagnetic dipoles:

$$\mathcal{E}_i \equiv \frac{e}{16\pi^2} (\psi \sigma^{\mu\nu} \nu_i) F_{\mu\nu}, \quad (i = 1, 2, 3);$$

- leptonic operators:

$$\begin{aligned} \tilde{\mathcal{N}}_{ijk} &\equiv (\psi \nu_i)(\nu_j \nu_k), \\ (i, j, k) &\in \{(1, 2, 2), (1, 3, 3), (1, 2, 3), (2, 1, 1), (2, 3, 3), (2, 1, 3), (3, 1, 1), (3, 2, 2)\}; \\ \mathcal{N}_{ijk} &\equiv (\bar{\psi} \bar{\sigma}^\mu \nu_i)(\bar{\nu}_j \bar{\sigma}_\mu \nu_k), \quad (1 \leq i \leq k \leq 3); \\ \mathcal{S}_{ijk}^{\nu e L} &\equiv (\psi \nu_i)(e_j^c e_k), \\ \mathcal{V}_{ijk}^{\nu e L} &\equiv (\bar{\psi} \bar{\sigma}^\mu \nu_i)(\bar{e}_j \bar{\sigma}_\mu e_k), \\ \mathcal{T}_{ijk}^{\nu e} &\equiv (\psi \sigma^{\mu\nu} \nu_i)(e_j^c \sigma_{\mu\nu} e_k), \quad (i = 1, 2, 3; \quad j, k = 1, 2); \end{aligned}$$

$$\tilde{\chi}_1^0 \rightarrow \gamma + \nu$$

(1-loop)

$$\begin{aligned} \tilde{\chi}_1^0 &\rightarrow \ell_1^\pm + \ell_2^\mp + \nu \\ \tilde{\chi}_1^0 &\rightarrow \nu_1 + \nu_2 + \nu_3 \end{aligned}$$

- semi-leptonic operators:

$$\begin{aligned}\mathcal{S}_{ijk}^{eq\,LL} &\equiv (\psi e_i)(d_j^c u_k), \\ \mathcal{S}_{ijk}^{eq\,RL} &\equiv (\bar{\psi} \bar{e}_i^c)(d_j^c u_k), \\ \mathcal{V}_{ijk}^{eq\,LL} &\equiv (\bar{\psi} \bar{\sigma}^\mu e_i)(\bar{d}_j \bar{\sigma}_\mu u_k), \\ \mathcal{V}_{ijk}^{eq\,RL} &\equiv (\psi \sigma^\mu \bar{e}_i^c)(\bar{d}_j \bar{\sigma}_\mu u_k), \\ \mathcal{T}_{ijk}^{eq\,L} &\equiv (\psi \sigma^{\mu\nu} e_i)(d_j^c \sigma_{\mu\nu} u_k),\end{aligned}$$

$$\begin{aligned}\mathcal{S}_{ijk}^{\nu u\,L} &\equiv (\psi \nu_i)(u_j^c u_k), \\ \mathcal{V}_{ijk}^{\nu u\,L} &\equiv (\bar{\psi} \bar{\sigma}^\mu \nu_i)(\bar{u}_j \bar{\sigma}_\mu u_k), \\ \mathcal{T}_{ijk}^{\nu u} &\equiv (\psi \sigma^{\mu\nu} \nu_i)(u_j^c \sigma_{\mu\nu} u_k), \\ \mathcal{S}_{ijk}^{\nu d\,L} &\equiv (\psi \nu_i)(d_j^c d_k), \\ \mathcal{V}_{ijk}^{\nu d\,L} &\equiv (\bar{\psi} \bar{\sigma}^\mu \nu_i)(\bar{d}_j \bar{\sigma}_\mu d_k), \\ \mathcal{T}_{ijk}^{\nu d} &\equiv (\psi \sigma^{\mu\nu} \nu_i)(d_j^c \sigma_{\mu\nu} d_k),\end{aligned}$$

$$\begin{aligned}\mathcal{S}_{ijk}^{eq\,LR} &\equiv (\psi e_i)(\bar{d}_j \bar{u}_k^c), \\ \mathcal{S}_{ijk}^{eq\,RR} &\equiv (\bar{\psi} \bar{e}_i^c)(\bar{d}_j \bar{u}_k^c), \\ \mathcal{V}_{ijk}^{eq\,LR} &\equiv (\bar{\psi} \bar{\sigma}^\mu e_i)(d_j^c \sigma_\mu \bar{u}_k^c), \\ \mathcal{V}_{ijk}^{eq\,RR} &\equiv (\psi \sigma^\mu \bar{e}_i^c)(d_j^c \sigma_\mu \bar{u}_k^c), \\ \mathcal{T}_{ijk}^{eq\,R} &\equiv (\bar{\psi} \bar{\sigma}^{\mu\nu} \bar{e}_i^c)(\bar{d}_j \bar{\sigma}_{\mu\nu} \bar{u}_k^c), \\ (i, j = 1, 2, k = 1); \\ \mathcal{S}_{ijk}^{\nu u\,R} &\equiv (\psi \nu_i)(\bar{u}_j \bar{u}_k^c), \\ \mathcal{V}_{ijk}^{\nu u\,R} &\equiv (\bar{\psi} \bar{\sigma}^\mu \nu_i)(u_j^c \sigma_\mu \bar{u}_k^k), \\ (i = 1, 2, 3, j, k = 1); \\ \mathcal{S}_{ijk}^{\nu d\,R} &\equiv (\psi \nu_i)(\bar{d}_j \bar{d}_k^c), \\ \mathcal{V}_{ijk}^{\nu d\,R} &\equiv (\bar{\psi} \bar{\sigma}^\mu \nu_i)(d_j^c \sigma_\mu \bar{d}_k^k), \\ (i = 1, 2, 3, j, k = 1, 2);\end{aligned}$$

$$\tilde{\chi}_1^0 \rightarrow M^\pm + \ell^\mp$$
  

$$\tilde{\chi}_1^0 \rightarrow M^0 + \nu$$